*Progress In Electromagnetics Research M, Vol. 95, 135–144, 2020*

# Flexible Metamaterial Electromagnetic Harvester Using Modified Split-Ring Resonator

**Mohammed M. Bait-Suwailam[1], Thamer S. Almoneef[2, *], and Saud M. Saeed[2]**

**Abstract**—In this paper, a flexible metamaterial-based electromagnetic harvester is proposed for wearable applications at microwave regime. The proposed harvesting structure is composed of a modified configuration from the conventional Split-Ring Resonator (SRR) inclusion and is printed on a grounded very thin flexible substrate. The proposed wearable harvester structure provides several interesting features, including its robustness, sustainability, and ease of integration with flexible electronics and sensors. Numerical full-wave studies are conducted, where results from a periodic arrangement of the proposed harvesting unit cell along with several two-dimensional arrays of harvesters are presented and discussed. Based on the numerical studies, the proposed electromagnetic harvesting structure exhibits good efficiency capability of power conversion from radio frequency received power to alternating-current harvested power across collecting loads above 90% for the three studied cases.

## 1. INTRODUCTION

The advancement in the research of electromagnetic energy harvesters has enabled wide range of applications such as remote sensing [1, 2], microwave energy scavenging [3–6], cell phone battery charging [7], Wireless Power Transfer (WPT) [8–11], Space Solar Power (SSP) [12, 13], the internet of things [14–17], and RFID's [18–20] to name a few. For the aforementioned applications, electromagnetic harvester can be built on a rigid substrate [21–25] or a flexible material [26–28], depending on the desired application. Recently, there have been much interest in wearable harvesters because they can be used in numerous applications that require conformity of the harvester, in addition to the increasing demand for higher data speeds and the requirements of continuous charging of electronic devices. In such applications, wearable harvesters fit well since they can supply the required power to a specific circuit. A great example is in health and fitness applications where wearable rectennas are used to capture electromagnetic waves which then can energise a sensor that can record vital readings such as body temperature, heart pulse, and breath [29]. Another life saving application includes powering a pacemaker to increase the reliability of the device and to ensure constant charging to its finite life battery [30]. Such wearable rectennas are usually built with allowable SAR (Specific Absorption Rate) levels to ensure that the radiation of the antenna does not have any health effect on the user [31, 32].

In this paper, we propose a flexible metamaterial harvesting structure using a modified unit cell from the well-known artificial inclusion, Split-Ring Resonator (SRR). Although classical SRR unit cell is a typical resonant inclusion that has been widely adopted in lots of applications, including electromagnetic absorbers and harvesters, we emphasize here that the proposed modified SRR allows for additional degree of freedom in introducing additional freedom in the placement of collective energy loads (i.e., rectifying diodes) to aid in achieving cost-effective channeling to the harvested energy instead of the use of the conventional SRR's cut gap or introducing additional complexity through conductive

*Received 14 May 2020, Accepted 21 July 2020, Scheduled 17 August 2020*

* Corresponding author: Thamer S. Almoneef (t.almoneef@psau.edu.sa).

[1] Department of Electrical and Computer Engineering, Sultan Qaboos University, Muscat, Oman. [2] Electrical Engineering Department, College of Engineering, Prince Sattam Bin Abdulaziz University, Al-Kharj, Saudi Arabia.

vias. Moreover, the proposed modified SRR provides practical solution to the placement of electronic components, i.e., diodes and/or varactors, which will result in proper connectivity at direct current (DC) as compared against conventional SRR when for instance a diode is placed at cut gap, which will result in short circuiting the diode at DC. Based on the aforementioned advantages from our proposed unit cell, it is believed that the developed modified SRR harvester structure will be valuable for many wearable applications, due to its sustainability and cost-effective solution when flexible electronics need to be integrated.

We present here comprehensive numerical results for the performance of the proposed flexible harvester by computing its efficiency, considering an infinitely large structure as well as several cases of finite harvesting structure, namely $3\times3$, $5\times5$, and $9\times9$ unit cells along $x$- and $y$-directions, respectively. In particular, we are mainly focusing on the conversion efficiency from an incident radio frequency (RF) power ($P_{\mathrm{RF}}$) that is available at the footprint of the harvester structure area to the collected one as an alternating-current (AC) power ($P_{\mathrm{AC}}$), i.e., namely, RF to AC conversion efficiency. The numerical full-wave simulations were carried out using the finite-integral solver of CST Microwave Studio. We highlight here that it is expected from measurements a drop in the efficiency compared to the simulated results. This is attributed mainly to the losses from the diodes during the rectification process, in which the resistive loads that are considered in simulation models will be replaced by diodes.

## 2. ELECTROMAGNETIC HARVESTER DESIGN

The proposed unit cell for the wearable electromagnetic harvester is depicted in Fig. 1. The unit cell comprises a metallic modified split-ring resonator (M-SRR) that is printed on the top of a grounded very thin flexible substrate. In order to minimize losses, a very low loss flexible dielectric substrate is considered (Rogers RT/duroid 5880 laminate, with a dielectric constant $\epsilon_r$ of 2.2, $\tan\delta = 0.0009$, and a thickness $h = 0.787\,\mathrm{mm}$). The optimized dimensions of the proposed square-shaped metamaterial electromagnetic harvester unit cell (see Fig. 1) are: length of $L = 18\,\mathrm{mm}$, $g_1 = 0.5\,\mathrm{mm}$, $g_2 = 0.4\,\mathrm{mm}$, $w_1 = 2.5\,\mathrm{mm}$, $w_2 = 1.5\,\mathrm{mm}$, and $w_3 = 0.6\,\mathrm{mm}$.

In order to quantify the robustness of the proposed harvesting energy collectors in utilizing the incident electromagnetic energy that is available within their footprint areas to useable AC power, the

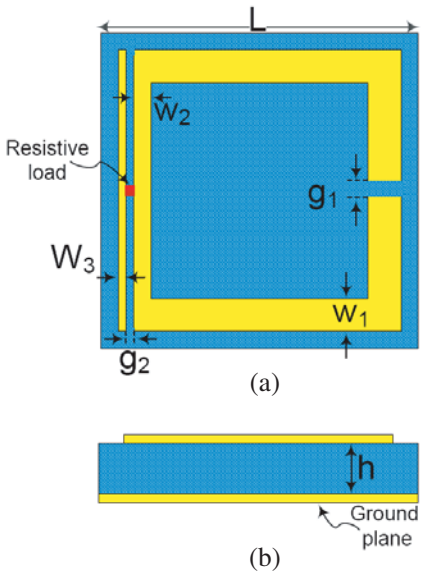


**Figure 1.** (a) Top view of the proposed wearable metamaterial electromagnetic harvester with details of its structure parameters; (b) side view of the proposed wearable harvester. Note that yellow shaded region represents metallization.

overall efficiency of proposed harvester structure is computed using

$$\eta = \frac{P_{\mathrm{AC}}}{P_{avg.}}, \tag{1}$$

where $P_{\mathrm{AC}}$ is the time-average AC power that is received by all terminated collectors (resistive loads), and $P_{avg.}$ is the total time-average incident power that is available at the footprint area of the terminated collectors. For more than one unit cell collector, $P_{\mathrm{AC}}$ can be calculated using

$$P_{\mathrm{AC}} = \sum_{k=1}^{n} \frac{V_k^2}{R_k} \tag{2}$$

where $R_k$ is the resistance of collector $k$, and $V_k$ is the AC voltage across $R_k$ of collector $k$.

### 2.1. Effect of Proposed Modified-SRR Harvester Unit Cell Parameters on Efficiency

In this part, we numerically investigate the effect of several physical parameters of the proposed modified SRR harvesting unit cell on the computed efficiency, namely: cut gap $g_1$ and resistive load gap $g_2$. For convenience, resistive load of $R_{load} = 450\,\Omega$ is considered. Within the numerical setup, a unit cell was placed within an air-filled waveguide, where the four adjacent side walls were enforced with perfect electric conductor (PEC) and perfect magnetic conductor (PMC) walls. A waveguide port was then launched from top of the air box. It is instructive to highlight here that these enforced boundary conditions mimicking an infinite arrangement are copied from the unit cell.

The effect of the modified SRR harvester unit cell cut gap, $g_1$, is studied first. Fig. 2 shows the efficiency of the harvester as $g_1$ is increased. Without the loss of generality, only four discrete values are considered for the cut gap. As can be seen from Fig. 2, there is only very minimal shift to the peak efficiency towards higher frequencies, while as cut gap, $g_1$ is increased, and peak efficiency remains almost the same at around 90% for the four cases of $g_1$.

Figure 3 depicts the effect of increasing the collector load gap, $g_2$, on the harvested energy. As can be seen, as the size of $g_2$ gap is increased, we observe a dramatic decay of harvested efficiency with a noticeable shift to efficiency peak towards higher frequencies. For instance, peak efficiency of nearly 90% was achieved for load gap $g_2 = 0.4\,\mathrm{mm}$ at a frequency of 4.46 GHz, with sudden decay and shift to peak efficiency for the case of load gap $g_2 = 1.6\,\mathrm{mm}$ and efficiency of around 74.7% at 5.1 GHz. This is explained as follows. Since the increase of $g_2$ gap will incur additional decrease to the overall capacitance of the harvester unit cell, a shift to peak efficiency towards higher frequencies is expected.

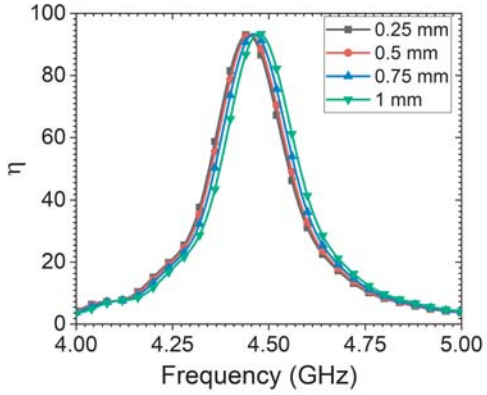


**Figure 2.** Parametric study showing the effect of modified SRR cut gap, $g_1$, on the harvested efficiency of the proposed harvesting unit cell.

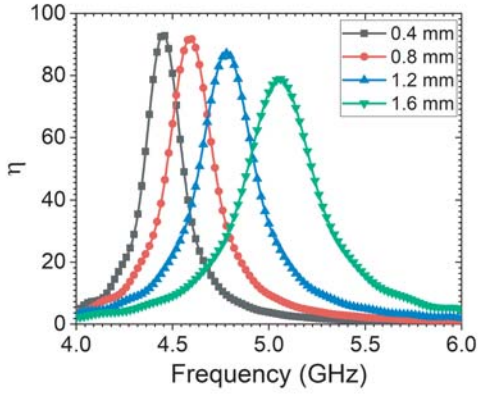


**Figure 3.** Parametric study showing the effect of modified SRR collector load gap, $g_2$, on the harvested efficiency of the proposed harvesting unit cell.

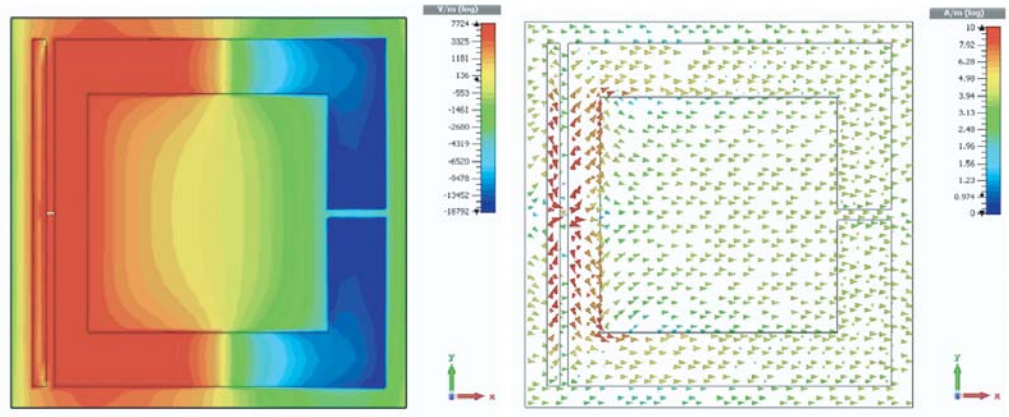

(a) (b)

**Figure 4.** (a) Electric field distribution, and (b) surface current distribution for the proposed modified SRR flexible harvester unit cell at a frequency of 4.45 GHz.

Moreover, the shift of peak efficiency values for the case of varying $g_2$ gap is more significant than the values for the case of varying cut gap $g_1$.

Figures 4(a), (b) depict the electric field and surface current distributions within the plane of the proposed flexible harvester unit cell, respectively. As can be seen, maximum electric field strength can be seen within the proposed location of the collector load, i.e., gap $g_2$. Moreover, the surface current distribution as shown in Fig. 4(b) shows maximal strength along the vicinity of the gap, which is attributed to displacement current. As such, the capacitive effect due to this gap $g_2$ is as expected more significant and dominant than the cut gap $g_1$.

In order to have more physical insight from the proposed unit cell structure, an equivalent circuit model was developed as shown in Fig. 5(a). For convenience, the presented circuit model is considered, although other circuit model topologies can also be adopted. Details of the circuit parameters and their extracted optimized values are tabulated in Table 1. Fig. 5(b) depicts comparison between the results that are obtained from the proposed harvester when collector load is replaced with a discrete port using numerical full-wave CST simulator and compared against the retrieved one from the proposed

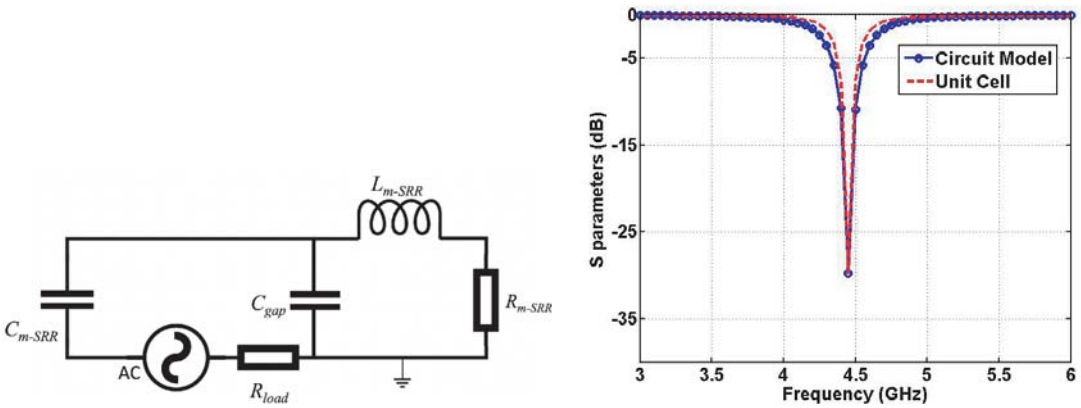


(a) (b)

**Figure 5.** (a) Equivalent circuit model of the proposed modified-SRR harvester unit cell structure, and (b) the retrieved reflection coefficient of the harvester when in transmission mode showing comparison between result from CST microwave studio and compared against the obtained one using ADS. Note that a collector load resistance of 450 Ω was considered.

**Table 1.** Equivalent circuit model of the proposed modified-SRR unit cell and its parameters.

| Circuit Parameters | Description | Extracted Value |
|---|---|---|
| $R_{m\text{-}SRR}$ | metallic and dielectric losses | 1 Ω |
| $L_{m\text{-}SRR}$ | iductance of the modified-SRR | 0.94 nH |
| $C_{m\text{-}SRR}$ | capacitance of the collector load gap, $g_2$ | 0.1 pF |
| $C_{gap}$ | capacitance of the cut gap, $g_1$ | 1.32 pF |
| $R_{load}$ | resistance of the collector load | 450 Ω |

equivalent circuit model using Agilent Design System (ADS) circuit simulator. Good agreement can be seen between results of the full-wave simulation and circuit model when the harvester is used in transmission mode.

### 2.2. Effect of Proposed Flexible Harvester Size on Efficiency

In this numerical study, two finite harvesters utilizing the proposed modified SRR unit cell are considered. The two finite-size harvesters have dimensions of $3 \times 3$ cells and $5 \times 5$ cells along $x$- and $y$-directions, respectively. The overall aperture area for the $3 \times 3$ geometry is 54-mm$^2$, while that for $5 \times 5$ cells is 90-mm$^2$.

Figure 6 shows a perspective view of the setup that was used to compute the efficiency numerically from the developed finite sized flexible harvesters. A plane wave was launched from the top of an air-filled computational space, while absorbing boundary conditions were applied along the rest of the side boundaries at a distance of half-wavelength away from the harvester's edges. Note that the proposed metamaterial harvester structure is backed with a metallic ground plane. As such, we are only interested in the reflectivity response from this very thin flexible metamaterial harvester structure upon excitation of an incident plane wave along with the harvested energy within the collector loads.

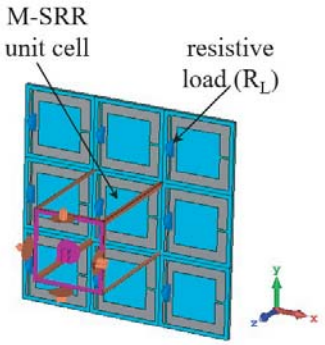


**Figure 6.** Perspective view of the numerical setup for the computation of the efficiency from the proposed electromagnetic flexible harvester. For convenience, a structure of $3 \times 3$ unit cells is displayed.

Figure 7 shows the computed efficiency from the proposed wearable harvester for the two finite-size harvesters of $3 \times 3$ and $5 \times 5$ and compared against a reference case of infinite arrangement from the unit cell. As can be seen, the case of $3 \times 3$ finite harvester achieved a conversion efficiency from RF to AC above 95%, while that for $5 \times 5$ harvester was around 90%. It is worth noting that the reference case of infinite arrangement of unit cell achieved an efficiency of around 78%. This is attributed to the coupling effect which was minimal for the $3 \times 3$ harvester as compared against the other two cases. Moreover, the aperture size for the $3 \times 3$ harvester is in fact larger than the physical area, which is not the case for the other two cases, in which aperture area for the $5 \times 5$ harvester is smaller than the aperture area for the $3 \times 3$ case. As a matter of fact, one should expect that the aperture area would be comparable to the physical area for the unit cell with infinite periodic arrangement, which mimics

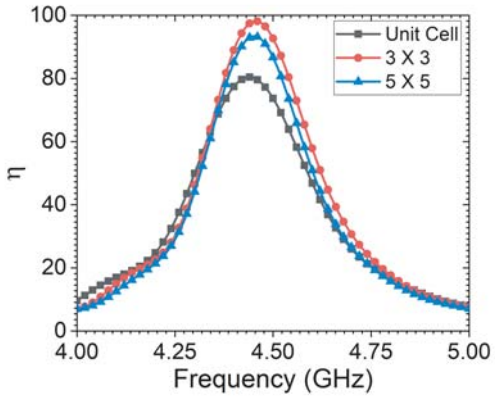


**Figure 7.** Numerical results showing the total collected efficiency from the proposed flexible microwave harvester of two finite sizes and compared against a reference case of infinite unit cell arrangement.

an infinite harvester. From the obtained results from these finite-size harvesters, the collected efficiency from such flexible harvesters is good enough for many wearable applications.

### 2.3. Effect of Bending on Performance of the Flexible Harvester

When the harvester is placed on wearables, it will most likely be exposed to bending effects due to the nature and the flexibility of the host wearer. Therefore, it is very essential to study the effect of bending the proposed harvester on the total conversion efficiency of the harvester. A numerical study was conducted, where the $3 \times 3$ and $5 \times 5$ harvesters were modeled in CST microwave studio, as shown in Fig. 8, with bending effect to all the three layers, namely: the resonator layer (i.e., modified SRR inclusions), flexible substrate, and ground plane. Without loss of generality, only two different bending scenarios were studied where the harvesters were wrapped and bent in partial cylindrical shape with radii of $R = 25\,\text{mm}$ in one case and $R = 50\,\text{mm}$ in another case (for comparison purposes) for both harvesters of $3 \times 3$ and $5 \times 5$ sizes as shown in Fig. 8.

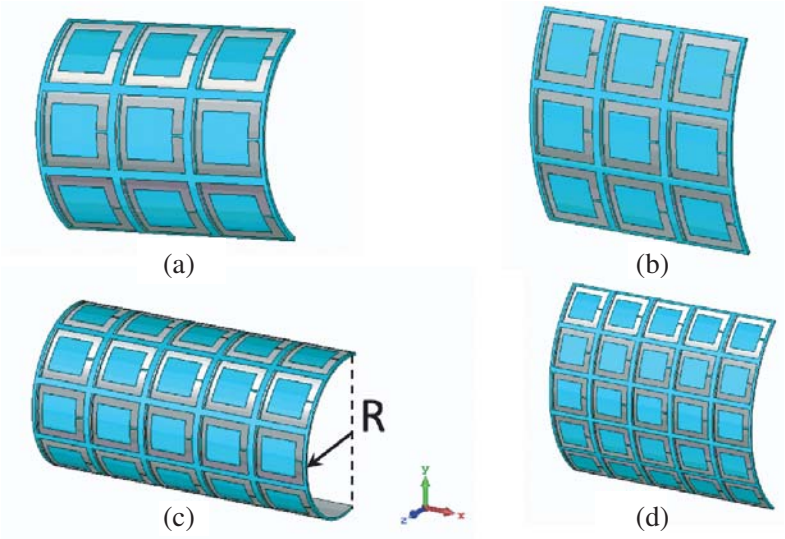


**Figure 8.** Perspective view of the proposed microwave metamaterial finite-size harvesters (a) $3 \times 3$ with cylindrical bending radius of $R = 25\,\text{mm}$; (b) $3 \times 3$ with bending radius of $R = 50\,\text{mm}$; (c) $5 \times 5$ with bending radius of $R = 25\,\text{mm}$; and (d) $5 \times 5$ with bending radius of $R = 50\,\text{mm}$.

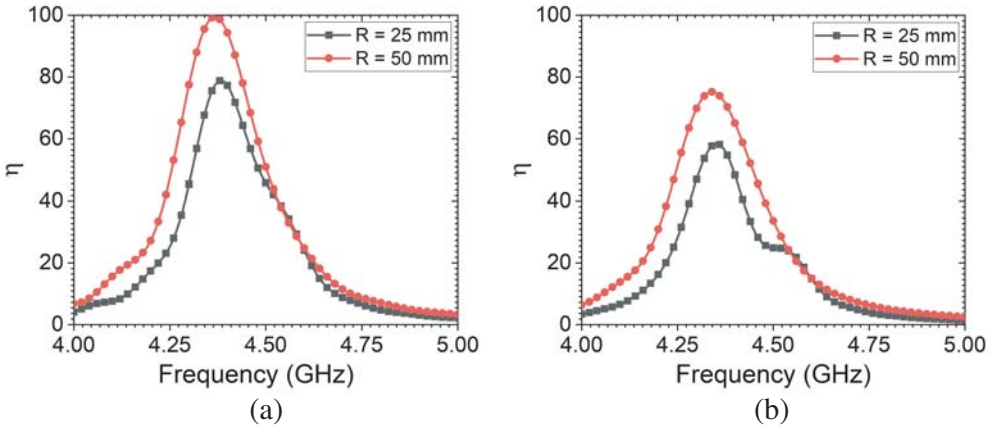


**Figure 9.** Numerical results showing the total collected efficiency from the proposed wearable microwave harvester under different bending scenarios for (a) the $3 \times 3$ harvester, and (b) the $5 \times 5$ harvester.

The efficiencies of the $3 \times 3$ and $5 \times 5$ harvesters for both bending scenarios are shown in Figs. 9(a), (b), respectively. As can be seen from Fig. 9(a), the efficiency from the $3 \times 3$ harvester was above 95% for the bending case of $R = 50\,\text{mm}$, which is almost the same as the flat case for the same harvester. However, when bending of $R = 25\,\text{mm}$ was applied to the $3 \times 3$ harvester, efficiency dropped to around 79%. The efficiency from the $5 \times 5$ harvester showed slight degradation as compared against the $3 \times 3$ harvester, as shown in Fig. 9(b). In fact, this is expected, due to the number of resonators that are in bending condition and that resulted in minimal collected energy by the resistive loads. Most importantly, the efficiency peaks exposed to very minimal shift as compared against the flat cases.

## 3. PROPOSED $9 \times 9$ FLEXIBLE METAMATERIAL HARVESTER

In this section, we investigate the case of a $9 \times 9$ flexible metamaterial harvester. The overall surface area of this proposed harvester is of size $162 \times 162\,\text{mm}^2$. Fig. 10 depicts the surface current distribution within the metallic modified SRR inclusions. As can be seen from the zoomed-in inset in Fig. 10, an in-phase surface current circulates within the two sides of the ring (i.e., top and bottom sides) and ends up at the collector load. Note that this current distribution within the inset corresponds to the center metallic ring of this $9 \times 9$ harvester. Moreover, we can observe as well from Fig. 10 strong current distribution within the vicinity of the center metallic modified SRR ring.

Figure 11 shows the calculated conversion efficiency from RF to AC power for the proposed $9 \times 9$ harvester when being flat and bent with a radius of $R = 50\,\text{mm}$. As can be seen from the figure, peak efficiency around 98% is observed, while the efficiency for the same harvester when being bent with $R = 50\,\text{mm}$ was around 48%. This is because of the effect of bending, which resulted in lower collected energy from the loads under normal incidence from plane wave.

One interesting study that was carried out is to ensure health safety when such a flexible harvester is attached within lossy human tissues for wearable applications. In other words, the Specific Absorption Rate (SAR) level from the proposed $9 \times 9$ electromagentic harvester when being attached to human tissues needs to be maintained below the allowable safety margins. In this study, we considered three lossy layers of human tissues, namely: skin (2 mm thick), fat (3 mm thick), and muscle (with 5 mm thickness), where properties of those tissues are embedded within CST Microwave Studio. The harvester is attached on top of those tissues without any air-gap spacing. A plane wave excitation was launched from far-field regime to the harvester. At end, the peak SAR was calculated that is averaged over 10-g of lossy tissue. Low SAR value was recorded, which was 0.44 W/Kg and is below 2.0 W/Kg according to International Electrotechnical Commission (IEC) standards for a 10-g average mass. Fig. 12 depicts the three dimensional pattern of the recorded maximum SAR level from this proposed harvester when being attached on lossy human tissues.

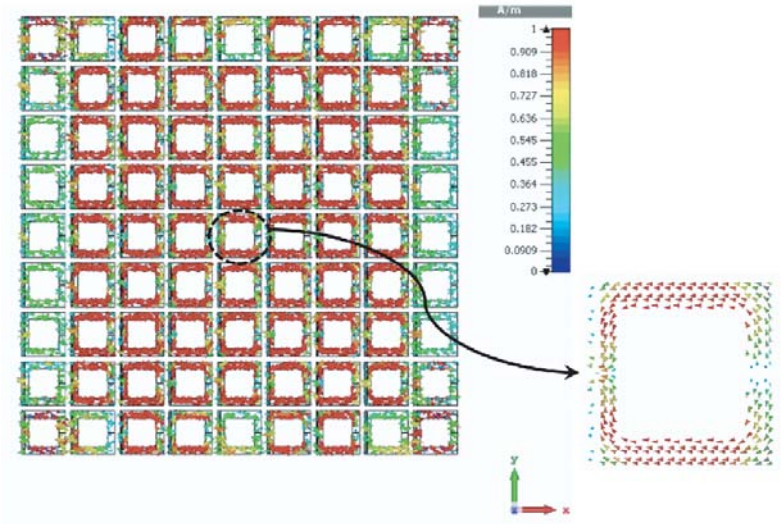


**Figure 10.** Surface current distribution for the proposed modified SRR flexible harvester of size $9 \times 9$ and a zoomed-in inset capture of surface current distribution within the central unit cell of the $9 \times 9$ flexible harvester.

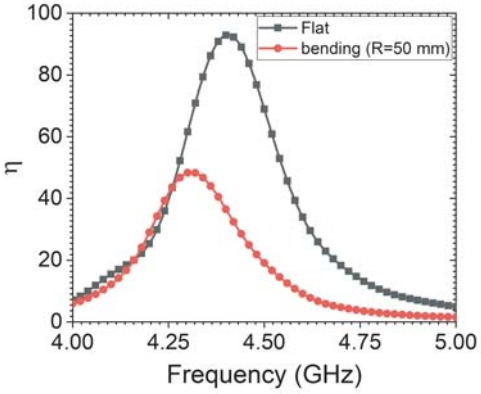


**Figure 11.** Numerical results showing the total collected efficiency from the proposed flexible microwave harvester for the $9 \times 9$ harvester when flat and when bent with radius of 50 mm.

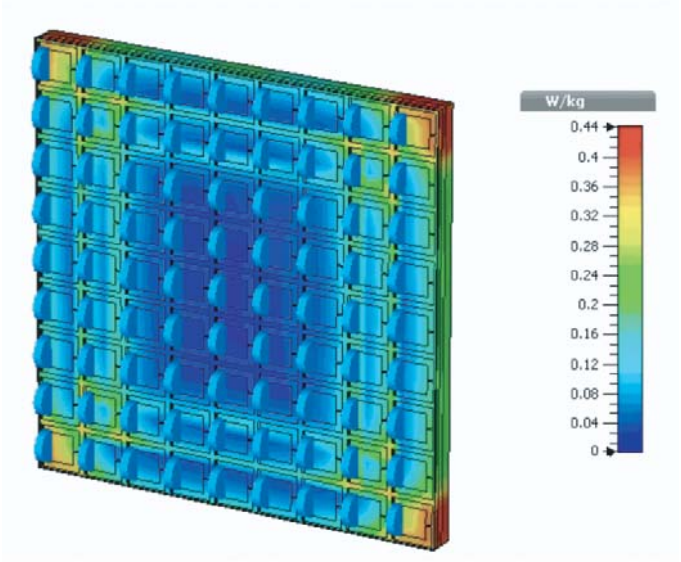


**Figure 12.** 3D snapshot showing the peak SAR pattern that is averaged over 10-g of tissue from the proposed flexible $9 \times 9$ harvester when attached to human tissues. Note that a 1-W power was assumed for the incident plane wave.

## 4. CONCLUSIONS

In this paper, a flexible metamaterial-based electromagnetic harvester was proposed. The developed metamaterial harvesting structure is based on a modified version of the conventional subwavelength split-ring resonator. Numerical full-wave studies were carried out in order to investigate the performance of this wearable harvester. Furthermore, the effect of the proposed harvester unit cell parameters on the RF-to-AC power conversion efficiency strength was analyzed. Several finite sizes from the proposed harvester unit cell were considered, and their performances were presented and discussed both in flat and bending scenarios.

Based on the numerical full-wave results, efficiency above 85% was maintained for the investigated finite-sized structures when being maintained flat. Sufficient conversion efficiency was obtained for the studied finite-sized harvesting structures in bent conditions. It was observed that efficiency starts to decay below 80% as more bending (i.e., $R < 50\,\text{mm}$) is applied to the harvesting structures, which can be considered as an extreme worst scenario. However, it is instructive to highlight here that despite slight degradation to efficiency of finite size harvesters when being exposed to bending, such conversion efficiency is still useful for many wearable applications.

It is worth noting here that efficiency of the finite harvesters needs to be tested in real-world. We highlight here that a minor drop to efficiency of proposed flexible metamaterial harvesters is expected, due to the losses from the diodes during the rectification process. Moreover, the inherent harmonics that are generated due to the nonlinear behavior of diodes will contribute to the minor drop to efficiency of the harvester. Other losses can result from the fabrication tolerances.

## ACKNOWLEDGMENT

The first author acknowledges the support of Sultan Qaboos University, Oman. This publication was supported by the Deanship of Scientific Research at Prince Sattam bin Abdulaziz University, Alkharj, Saudi Arabia.

## REFERENCES

1. Jiang, S. and S. V. Georgakopoulos, "Optimum wireless powering of sensors embedded in concrete," *IEEE Transactions on Antennas and Propagation*, Vol. 60, No. 2, 1106–1113, 2011.
2. Shams, K. M. and M. Ali, "Wireless power transmission to a buried sensor in concrete," *IEEE Sensors Journal*, Vol. 7, No. 12, 1573–1577, 2007.
3. Assimonis, S. D., V. Fusco, A. Georgiadis, and T. Samaras, "Efficient and sensitive electrically small rectenna for ultra-low power RF energy harvesting," *Scientific Reports*, Vol. 8, No. 1, 1–13, 2018.
4. Shen, S., C.-Y. Chiu, and R. D. Murch, "Multiport pixel rectenna for ambient RF energy harvesting," *IEEE Transactions on Antennas and Propagation*, Vol. 66, No. 2, 644–656, 2017.
5. Andersson, M. A., A. Özçelikkale, M. Johansson, U. Engström, A. Vorobiev, and J. Stake, "Feasibility of ambient RF energy harvesting for self-sustainable M2M communications using transparent and flexible graphene antennas," *IEEE Access*, Vol. 4, 5850–5857, 2016.
6. Piñuela, M., P. D. Mitcheson, and S. Lucyszyn, "Ambient RF energy harvesting in urban and semi-urban environments," *IEEE Transactions on Microwave Theory and Techniques*, Vol. 61, No. 7, 2715–2726, 2013.
7. Apostolos, J. T., J. D. Logan, and W. Mouyos, "Low frequency rectenna system for wireless charging," US Patent App. 16/569,814, January 2, 2020.
8. Takeno, K., "Wireless power transmission technology for mobile devices," *IEICE Electronics Express*, Vol. 10, No. 21, 20132010–20132010, 2013.
9. Shinohara, N., "Rectennas for microwave power transmission," *IEICE Electronics Express*, Vol. 10, No. 21, 20132009–20132009, 2013.
10. Ashoor, A. Z., T. S. Almoneef, and O. M. Ramahi, "A planar dipole array surface for electromagnetic energy harvesting and wireless power transfer," *IEEE Transactions on Microwave Theory and Techniques*, Vol. 66, No. 3, 1553–1560, 2017.
11. Suh, Y.-H. and K. Chang, "A high-efficiency dual-frequency rectenna for 2.45-and 5.8-GHz wireless power transmission," *IEEE Transactions on Microwave Theory and Techniques*, Vol. 50, No. 7, 1784–1789, 2002.
12. Glaser, P. E., "Power from the sun: Its future," *Science*, Vol. 162, No. 3856, 857–861, 1968.
13. Erb, R., "Power from space — The tough questions: The 1995 Peter E. Glaser lecture," *Acta Astronautica*, Vol. 38, Nos. 4–8, 539–550, 1996.

14. Shafique, K., B. A. Khawaja, M. D. Khurram, S. M. Sibtain, Y. Siddiqui, M. Mustaqim, H. T. Chattha, and X. Yang, "Energy harvesting using a low-cost rectenna for Internet of Things (IoT) applications," *IEEE Access*, Vol. 6, 30932–30941, 2018.
15. Lin, W. and R. W. Ziolkowski, "A circularly polarized wireless power transfer system for internet-of-things (IoT) applications," *2020 4th Australian Microwave Symposium (AMS) IEEE*, 1–2, 2020.
16. Singh, N., S. Kumar, and B. K. Kanaujia, "A new trend to power up next-generation Internet of Things (IoT) devices: 'rectenna'," *Energy Conservation for IoT Devices*, 331–356, Springer, 2019.
17. Eid, A., J. G. Hester, J. Costantine, Y. Tawk, A. H. Ramadan, and M. M. Tentzeris, "A compact source-load agnostic flexible rectenna topology for IoT devices," *IEEE Transactions on Antennas and Propagation*, Vol. 68, No. 4, 2621–2629, 2019.
18. Michisaka, T., et al., "Novel sensing techniques of chipless RFID sensor for infrastructure," *IEICE Communications Express*, 2020.
19. Yang, S., M. Crisp, R. V. Penty, and I. H. White, "RFID Enabled Health Monitoring System for Aircraft Landing Gear," *IEEE Journal of Radio Frequency Identification*, Vol. 2, No. 3, 159–169, 2018.
20. Jauregi, I., H. Solar, A. Beriain, I. Zalbide, A. Jimenez, I. Galarraga, and R. Berenguer, "UHF RFID temperature sensor assisted with body-heat dissipation energy harvesting," *IEEE Sensors Journal*, Vol. 17, No. 5, 1471–1478, 2016.
21. Sun, H., Y.-X. Guo, M. He, and Z. Zhong, "A dual-band rectenna using broadband Yagi antenna array for ambient RF power harvesting," *IEEE Antennas and Wireless Propagation Letters*, Vol. 12, 918–921, 2013.
22. Almoneef, T. S., F. Erkmen, and O. M. Ramahi, "Harvesting the energy of multi-polarized electromagnetic waves," *Scientific Reports*, Vol. 7, No. 1, 1–14, 2017.
23. Lu, P., C. Song, and K. M. Huang, "A compact rectenna design with wide input power range for wireless power transfer," *IEEE Transactions on Power Electronics*, Vol. 35, No. 7, 6705–6710, 2020.
24. Lu, P., C. Song, F. Cheng, B. Zhang, and K. M. Huang, "A self-biased adaptive reconfigurable rectenna for microwave power transmission," *IEEE Transactions on Power Electronics*, 2020.
25. Sun, H., H. He, and J. Huang, "Polarization-insensitive rectenna arrays with different power combining strategies," *IEEE Antennas and Wireless Propagation Letters*, Vol. 19, No. 3, 492–496, 2020.
26. Vital, D., S. Bhardwaj, and J. L. Volakis, "Textile based large area RF-power harvesting system for wearable applications," *IEEE Transactions on Antennas and Propagation*, 2019.
27. Monti, G., L. Corchia, and L. Tarricone, "UHF wearable rectenna on textile materials," *IEEE Transactions on Antennas and Propagation*, Vol. 61, No. 7, 3869–3873, 2013.
28. Palazzi, V., J. Hester, J. Bito, F. Alimenti, C. Kalialakis, A. Collado, P. Mezzanotte, A. Georgiadis, L. Roselli, and M. M. Tentzeris, "A novel ultra-lightweight multiband rectenna on paper for RF energy harvesting in the next generation LTE bands," *IEEE Transactions on Microwave Theory and Techniques*, Vol. 66, No. 1, 366–379, 2017.
29. Lin, C.-H., C.-W. Chiu, and J.-Y. Gong, "A wearable rectenna to harvest low-power RF energy for wireless healthcare applications," *2018 11th International Congress on Image and Signal Processing, BioMedical Engineering and Informatics (CISP-BMEI) IEEE*, 1–5, 2018.
30. Asif, S. M., A. Iftikhar, J. W. Hansen, M. S. Khan, D. L. Ewert, and B. D. Braaten, "A novel RF-powered wireless pacing via a rectenna-based pacemaker and a wearable transmit-antenna array," *IEEE Access*, Vol. 7, 1139–1148, 2018.
31. Ahmed, M. I., M. F. Ahmed, A.-E. H. Shaalan, et al., "SAR calculations of novel wearable fractal antenna on metamaterial cell for search and rescue applications," *Progress In Electromagnetics Research*, Vol. 53, 99–110, 2017.
32. Il Kwak, S., D.-U. Sim, J. H. Kwon, and Y. J. Yoon, "Design of PIFA with metamaterials for body-SAR reduction in wearable applications," *IEEE Transactions on Electromagnetic Compatibility*, Vol. 59, No. 1, 297–300, 2016.